Int. J. Oral Maxillofac. Surg. 2017; xxx: xxx–xxx
http://dx.doi.org/10.1016/j.ijom.2017.07.004, available online at http://www.sciencedirect.com

International Journal of Oral & Maxillofacial Surgery

Clinical Paper
Pre-Implant Surgery

Virtual quad zygoma implant placement using cone beam computed tomography: sufficiency of malar bone volume, intraosseous implant length, and relationship to the sinus according to the degree of alveolar bone atrophy

J. Bertos Quílez, R. Guijarro-Martínez, S. Aboul-Hosn Centenero, F. Hernández-Alfaro
Department of Oral and Maxillofacial Surgery, International University of Catalonia, Sant Cugat del Vallés, Barcelona, Spain

J. Bertos Quílez, R. Guijarro-Martínez, S. Aboul-Hosn Centenero, F. Hernández-Alfaro: Virtual quad zygoma implant placement using cone beam computed tomography: sufficiency of malar bone volume, intraosseous implant length, and relationship to the sinus according to the degree of alveolar bone atrophy. Int. J. Oral Maxillofac. Surg. 2017; xxx: xxx–xxx.

Abstract. The objective of this study was to investigate the malar bone volume and length that a zygomatic implant can engage, and the relationship to the sinus according to the degree of alveolar bone atrophy. A three-dimensional evaluation was performed using cone beam computed tomography scans from 23 patients with a totally edentulous maxilla; quad zygoma implants were virtually placed. The predictor variable was the amount of malar bone volume and length that a zygomatic implant can engage. The primary outcome variable was the relationship to the sinus according to the degree of alveolar bone atrophy. Other variables were the residual alveolar bone height to the floor of the sinus and the nasal cavity. The mean volume of malar bone engaged in this sample of 92 zygomatic implants was 0.19 ± 0.06 cm^3. The implant had an extrasinus path in 60.9% of cases, a parasinus path in 25%, and an intrasinus path in 14.1%. The results suggest that the average volume of malar bone engaged by a zygomatic implant is constant regardless of implant position and the degree of alveolar bone atrophy. As alveolar atrophy increases, the trajectory of the implant becomes more parasinus and intrasinus. The

0901-5027/000001+010

examiners were able to find enough bone to adequately distribute the implants in all cases.

Key words: zygoma implant; malar bone volume engaged; zygoma implant path; zygoma implant relationship to the sinus.

Accepted for publication

Since the introduction of zygoma implants by Brånemark in the 1990s[1], several technical modifications have been proposed in response to the disadvantages observed[2–4]. These disadvantages relate to the path of the implant, in which the platform emerges in the palatal cortical bone of the alveolar crest, thus rendering prosthetic rehabilitation uncomfortable, not only for the clinician but also for the patient. It is well acknowledged that a palatal emergence of a zygomatic implant implies compromised cleaning and diction, which in turn lead to a suboptimal rehabilitation for the patient[5].

With the aim of resolving this problem, the placement of zygoma implants is now prosthetically driven, and the emergence of the platform, as well as the path that the implant takes, has been modified. The placement of the implant platform in a more suitable position for rehabilitation has altered the relationship between the implant and the sinus, with the implant being outside the sinus (extrasinus) in most cases[6,7]. This has also changed the relationship between the implant platform and the residual alveolar crest. In fact, this relationship is sometimes non-existent depending on the class of alveolar bone atrophy, as described in the literature[8].

A number of study groups have focused on the surgical technique and subsequent modifications[4,9], number of implants per quadrant, and surgical and prosthetic complications[10], but little is known about the path of a zygomatic implant and its relationship to the alveolar crest[11].

In this context, the main objective of the present study was to investigate the amount of malar bone volume and length that a zygomatic implant can engage, and the expected relationship of the implant to the sinus depending on the degree of alveolar bone atrophy.

Materials and methods

The Research Ethics Committee of the International University of Catalonia approved this study. Every precaution was taken to protect the privacy of the research subjects and the confidentiality of their personal information.

Radiological sample

The cone beam computed tomography (CBCT) scans of a sample of 23 patients with a totally edentulous maxilla were collected. These CBCT scans had originally been taken for diagnostic purposes. The patients were recruited from the databases of the International University of Catalonia and the Institute of Maxillofacial Surgery at the Teknon Medical Centre (Barcelona). The CBCT scans were obtained with an i-CAT Cone Beam 3D Imaging device (Imaging Sciences International, Inc., Hatfield, PA, USA) with settings of 120 kVp, 8 mA, voxel size 0.4 mm, and a field of view of 27 × 14 cm.

Inclusion criteria

Patients with a fully edentulous maxilla and with alveolar bone atrophy due to tooth loss corresponding to class IV or V of the classification of Cawood and Howell were recruited[12]. Patients in whom tooth loss had occurred as a result of maxillofacial trauma or oncological resection surgery were excluded. Furthermore, patients with alveolar bone atrophy of class VI of the Cawood and Howell classification were also excluded.

Determination of the type of bone atrophy (Cawood and Howell classification)

The classification of alveolar bone atrophy was determined according to the reference points used in the study by Cawood and Howell[12] (Fig. 1).

A variable point ‘C’ (crest of the alveolar process) and two constant points marked at the limit between the basal bone and the alveolar bone labelled ‘I’ (incisive foramen) for the anterior maxilla and ‘GP’ (greater palatine foramen) for the posterior maxilla were identified. The distance between ‘I’ and ‘C’ and between ‘GP’ and ‘C’ allowed the determination of the precise type of alveolar bone atrophy.

A residual knife-edge ridge form that was inadequate in width and greater than 5 mm in height was categorized as class IV alveolar bone atrophy, and a residual flat-ridge ridge form that was inadequate in width and less than 5 mm in height without evident basilar loss was categorized as class V alveolar bone atrophy.

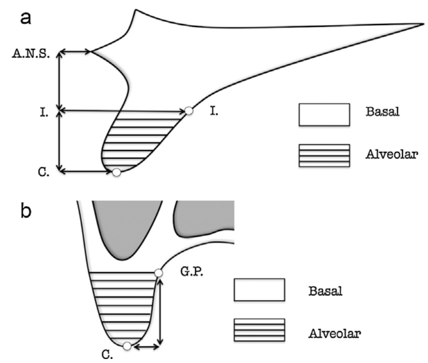

Fig. 1. Determination of alveolar bone atrophy according to the classification of Cawood and Howell: (a) the anterior sector; (b) the posterior sector.

Sample preparation

Simplant Pro 16.0 software (Simplant, Dentsply Sirona, Iberia) was used to simulate zygomatic implant placement. This process begins with the selection of an area of interest mask and the exclusion of the remaining CBCT data in order to make virtual implant planning simpler.

The mask limits were set as follows (Fig. 2): (1) the anterior limit was set in the coronal plane and was located at the level of the anterior nasal spine (ANS); (2) the posterior limit was set in the coronal plane and was located immediately distal

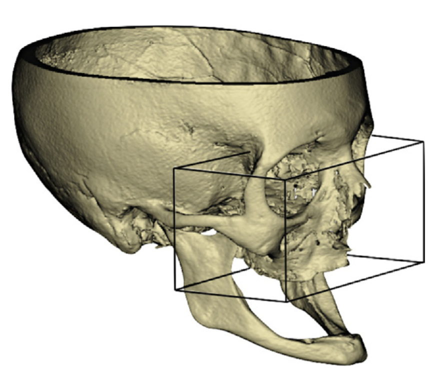

Fig. 2. Delimitation of the mask in a 3D model.

to the pterygoid plates; (3) the cranial limit was set in the axial plane and was located at nasion; (4) the caudal limit was set in the axial plane and was located immediately inferior to the alveolar crest of the upper maxilla; (5) the lateral limits were set in the sagittal plane and were located at the zigion points bilaterally.

A defined specific type of tissue to be included in the mask was set with the thresholding tool, which uses the Hounsfield unit (HU) level. This level ranges from a minimum of 250 HU to a maximum of 3071 HU, which is established by default as bone. Once the mask and the type of tissue were defined, a high quality 3D model was created.

Virtual implant planning

Four zygoma implants were virtually placed in each case. The panoramic curve was used as the basis for panoramic and sectional view calculations of implant placement. Once this step had been accomplished, zygoma implants were planned according to the anatomical insertion guidelines of Rossi et al. and Rigolizzo et al.[13,14] (Figs 3 and 4).

The specific position (anterior or posterior) and quadrant (first or second) of each zygomatic implant were described using the following nomenclature: Z1 was the first quadrant anterior implant, corresponding to the approximate position of the upper right lateral incisor (#12) or upper right canine (#13); Z2 was the first quadrant posterior implant, corresponding to the approximate position of the upper right first or second premolar (#14 or #15); Z3 was the second quadrant anterior implant, corresponding to the approximate position of the upper left lateral incisor (#22) or the upper left canine (#23); Z4 was the second quadrant posterior implant, corresponding to the approximate position of the upper left first or second premolar (#24 or #25).

Volume of malar bone engaged by the implant

The 'draw a volume' tool enabled the alignment of the implant perimeter in the axial, sagittal, and coronal planes along the portion of the zygoma implant located within the malar bone. Once every section of the implant had been aligned, a high-quality 3D model (the highest possible quality that the software can create) representing the volume of malar bone engaged by the zygoma implant (in cubic centimetres, cm^3) was generated. The software also provided the mean HU value for this portion of bone (Figs 5 and 6).

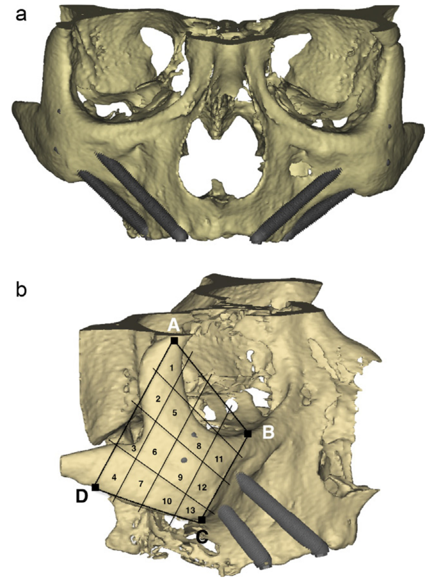

Fig. 3. 3D model of the mask. (a) Front view of four zygoma implants placed, two per quadrant, according to the anatomical insertion guidelines of Rossi et al. 2008. For the anterior implants (Z1 and Z3), the initial drilling point is the lowermost point of the alveolar crest, taking a line from the lateral margin of the nasal incisure; the final drilling point is the lowermost point on the lateral margin of the orbital socket. For the posterior implants (Z2 and Z4), the initial drilling point is the lowermost point of the alveolar crest, taking a line at a tangent to the lateral margin of the infraorbital foramen; the final drilling point is located one-third of the distance between the lowermost point of the lateral margin of the orbital socket and the lowermost point of the zygomaticomaxillary suture. (b) Three-quarter view of first quadrant implants Z1 and Z2 according to the anatomical anchorage guidelines of Rigolizzo et al. 2005. Sections 5, 6, 8, and 9 are described as the sections with the best potential for implant anchorage. In this case, implants are anchored in sections 8 and 9.

Relationship of the zygoma implant to the sinus according to the degree of alveolar bone atrophy

Along its path, the implant is associated with the maxillary sinus in different ways. Specific reference points were defined to establish which portions of the implant were associated with the sinus and in what way. These points were located at the intersection of two axes or lines (Figs 7 and 8).

All measurements were performed on two-dimensional (2D) CBCT images. The 'see the centric implant image' tool enabled the evaluation of the implant in its longitudinal axis and its relationship with the maxillary sinus.

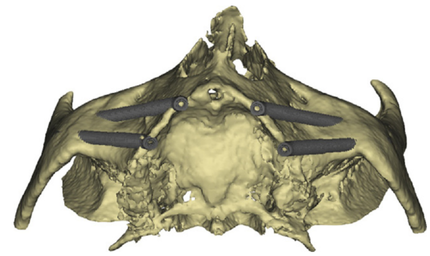

Fig. 4. 3D model of the mask. Occlusal view, in which the ideal emergence of the prosthetic implants is in the alveolar ridge. Anterior implants Z1 and Z3 emerge in an upper lateral incisor/canine position and posterior implants Z2 and Z4 emerge in an upper first or second premolar position.

The reference lines on a 2D image are shown in Fig. 7. These included the implant longitudinal axis and lines parallel to the axial plane.

The reference points are shown in Fig. 8. These were Z_a, corresponding to the implant apex; Z_b, following the im-

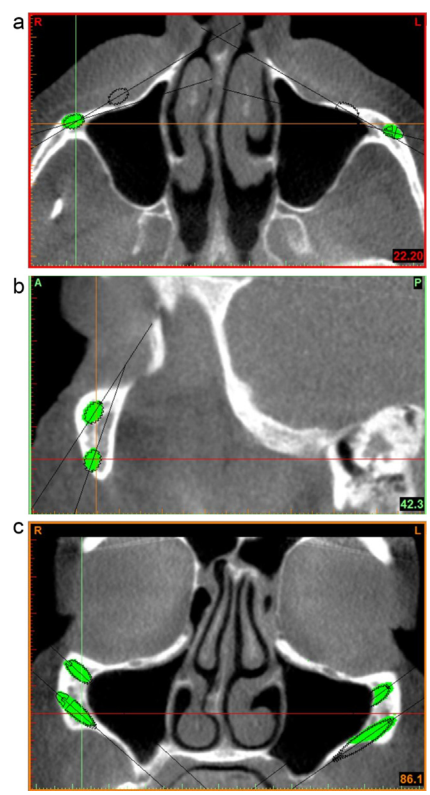

Fig. 5. 2D images in the (a) frontal, (b) axial, and (c) sagittal planes, in which the delimitation (in green) of each section of the zygoma implants can be seen. These were used to calculate the volume of malar bone engaged.

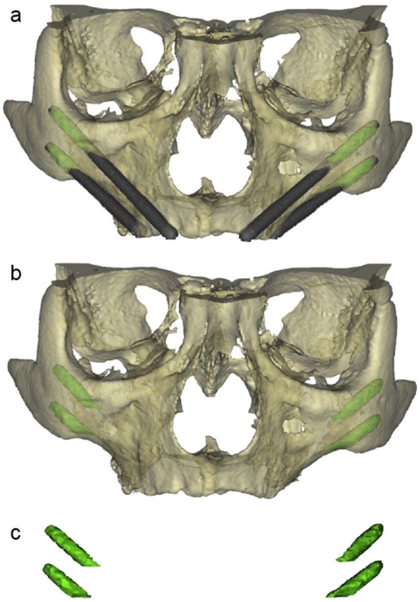

Fig. 6. Sequence of 3D images showing the volume of malar bone engaged by the zygoma implants. (a) The implants placed and the malar bone volume engaged highlighted in green, surrounding approximately the apical third. (b) To determine the volume of malar bone engaged, the implants are first hidden. (c) The mask is then hidden so that only the malar bone volume engaged by the zygoma implants can be seen.

plant insertion path, corresponding to the intersection between its longitudinal axis and a line parallel to the axial plane at the level where the implant penetrates the malar bone; Z_c, following the implant insertion path, corresponding to the intersection between its longitudinal axis and a line parallel to the axial plane at the level

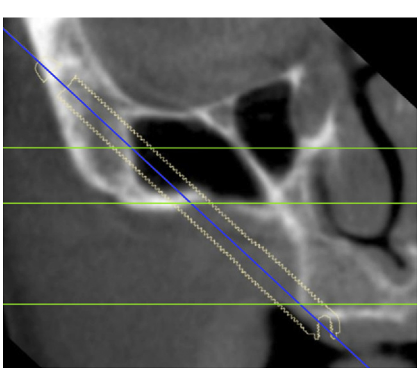

Fig. 7. Linear references on a 2D image: longitudinal axis of the implant (blue) and lines parallel to the axial plane (green). (For interpretation of the references to colour in this figure legend, the reader is referred to the web version of this article.)

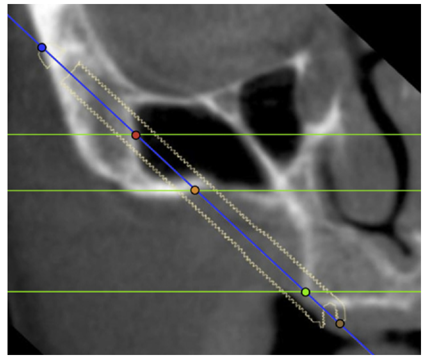

Fig. 8. Reference points on a 2D image: point Z_a (blue point), point Z_b (red point), point Z_c (orange point), point Z_d (green point), and point Z_e (brown point). (For interpretation of the references to colour in this figure legend, the reader is referred to the web version of this article.)

where the implant penetrates the maxillary sinus; Z_d, following the implant insertion path, corresponding to the intersection between its longitudinal axis and a line parallel to the axial plane at the level where the implant leaves the alveolar ridge; and Z_e, corresponding to the implant platform.

The intra-malar length (length of the implant within the malar bone) was defined as the distance between Z_a and Z_b. The intrasinus length was defined as the distance between Z_b and Z_c. The parasinus length was defined as the distance between Z_b or Z_c and Z_d or Z_e. The extrasinus length was defined as the distance between Z_b or Z_c and Z_d or Z_e.

When categorizing the path of each implant as intrasinus, parasinus, or extrasinus, it was established that the implant had to have at least 50% of its diameter associated with the maxillary sinus as follows: (1) extrasinus path: the implant is outside the maxillary sinus and has no contact with the lateral wall, or this contact is at most less than the lateral 50% of its diameter (Figs 9 and 10); (2) parasinus path: the implant is in contact with the lateral wall of the maxillary sinus in 50% (either lateral or medial) of its diameter (Figs 11 and 12); (3) intrasinus path: the implant is inside the maxillary sinus without any contact with the lateral wall or at most less than 50% of its diameter (Figs 13 and 14).

After measuring the intrasinus, parasinus, and/or extrasinus portions of the implant, the longest portion determined the category of path for the zygomatic implant (Fig. 15).

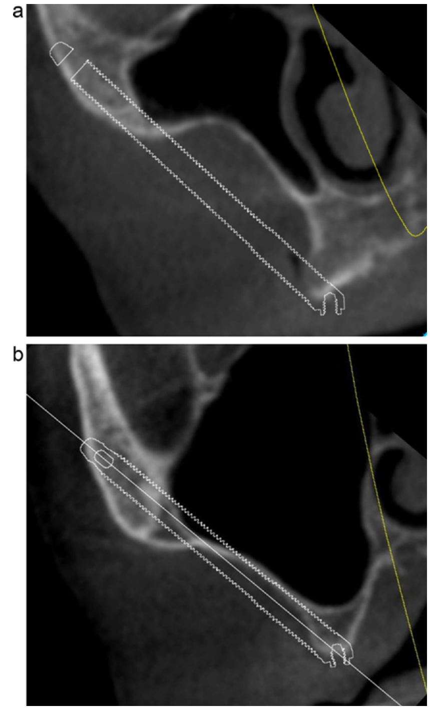

Fig. 9. Implants Z1 and Z2 with an extrasinus path: (a) Z1 implant showing no relationship with the lateral wall of the upper maxilla; (b) Z2 implant showing a relationship with the lateral wall of the upper maxilla and also with the maxillary sinus.

Measurement of the residual bone height to the floor of the maxillary sinus and the nasal cavity

A cross-section in which the entire implant platform could be adequately visualized was identified. The 'measure distance' tool was used to measure the linear distance between the most caudal point of the alveolar crest and the most caudal point of

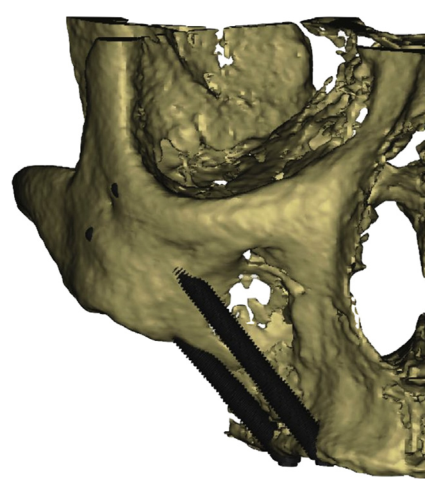

Fig. 10. 3D image of the Z1 and Z2 implants seen in Fig. 9.

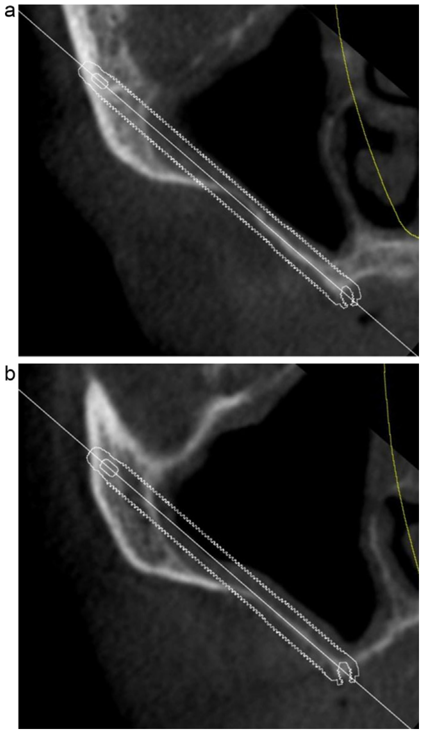

Fig. 11. (a) Z1 implant and (b) Z2 implant with a parasinus path. The implants relate totally with the lateral wall of the upper maxilla, passing through the maxillary sinus to anchor in the malar bone.

the maxillary sinus in the case of a Z2 or Z4 implant, or of the nasal fossa in the case of a Z1 or Z3 implant (Fig. 16).

Statistical analysis

The Student *t*-test for independent samples was used to compare the mean values of a given dimension according to the bone atrophy group. Prior to this, the normality of the data was corroborated with the Kolmogorov–Smirnov test. The result of

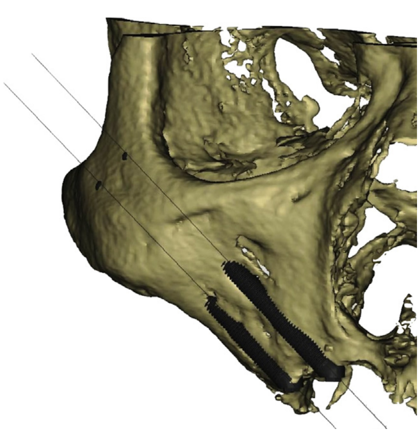

Fig. 12. 3D image of the Z1 and Z2 implants seen in Fig. 11.

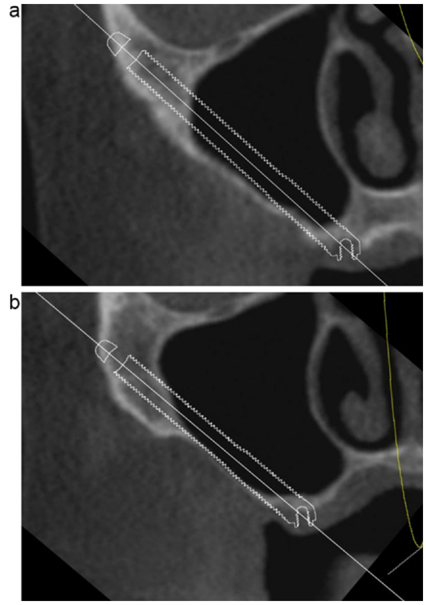

Fig. 13. (a) Z1 implant and (b) Z2 implant with an intrasinus path. The implants travel totally inside the maxillary sinus to anchor in the malar bone.

the *t*-test was validated, ensuring the homogeneity of the variances with Levene's test; Welch's correction was applied in the case of deviation.

The Kruskal–Wallis test was used to study the distribution of alveolar bone atrophy classes according to the different paths followed by the zygoma implants. The association χ^2 test was used to evaluate the degree of dependence between two categorical variables, such as implant path and degree of bone atrophy. For all tests, statistical significance was set at 0.05.

Results

Volume of malar bone engaged by a zygoma implant

For the sample of 92 zygoma implants, the mean volume of malar bone engaged by a zygoma implant was 0.19 ± 0.06 cm^3. The mean volume of malar bone engaged according to the implant position (anterior or posterior) is shown in Table 1. In the anterior sector ($n = 46$ anterior implants), the mean volume of malar bone engaged by the implant was 0.18 ± 0.05 cm^3. Stratified according to the Cawood and Howell classification of alveolar bone atrophy, the average volume of malar bone engaged was 0.18 ± 0.05 cm^3 in class IV and 0.19 ± 0.06 cm^3 in class V. In the posterior sector ($n = 46$ posterior implants), the mean volume of malar bone

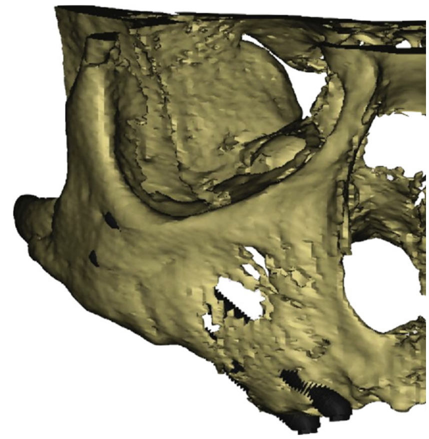

Fig. 14. 3D image of the Z1 and Z2 implants seen in Fig. 13.

engaged by the implant was 0.20 ± 0.06 cm^3. Stratified according to the Cawood and Howell classification of alveolar bone atrophy, the average volume of malar bone engaged was 0.21 ± 0.06 cm^3 in class IV and 0.19 ± 0.06 cm^3 in class V.

On comparing the volume of malar bone engaged between class IV and class V bone atrophy cases, no statistically significant difference was found overall ($P = 0.650$), or for the anterior and posterior locations separately ($P = 0.559$ and $P = 0.184$ for anterior and posterior, re-

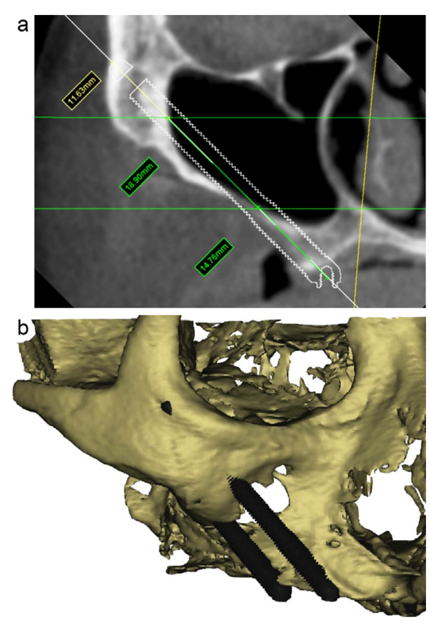

Fig. 15. (a) 2D image of a Z2 implant: the intrasinus portion of 18.90 mm is greater in length than the extrasinus portion of 14.76 mm. (b) 3D image of the same Z2 implant, which clinically seems to have an extrasinus path.

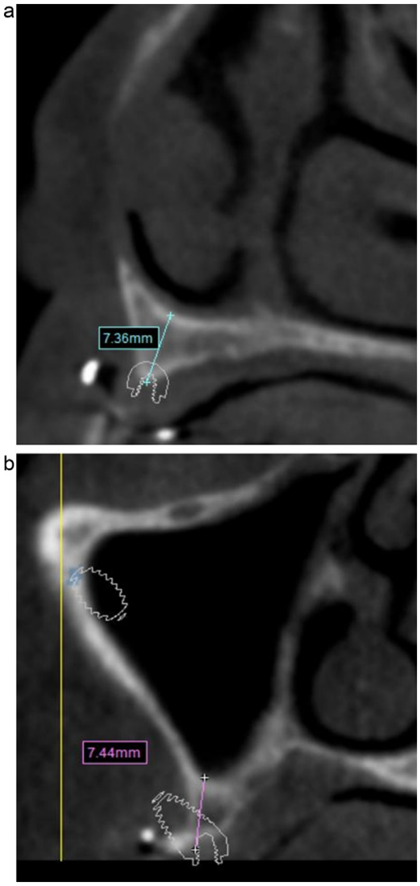

Fig. 16. (a) Distance to the floor of the maxillary sinus from the alveolar crest. (b) Distance to the floor of the nasal cavity from the alveolar crest.

Table 2. Volume of malar bone (cm^3) engaged by the zygoma implant according to the sector (anterior and posterior) and the Cawood and Howell classification of alveolar bone atrophy (classes IV and V).[a]

	Class IV	Class V	*P*-value[b]
Total	0.19 ± 0.05 (0.18–0.21)	0.19 ± 0.06 (0.17–0.21)	0.650
Anterior sector	0.18 ± 0.05 (0.16–0.20)	0.19 ± 0.06 (0.16–0.22)	0.559
Posterior sector	0.21 ± 0.06 (0.19–0.24)	0.19 ± 0.06 (0.17–0.21)	0.184

[a] Results are presented as the mean ± standard deviation (95% confidence interval).
[b] The *t*-test was used to compare the means according to the degree of alveolar bone atrophy.

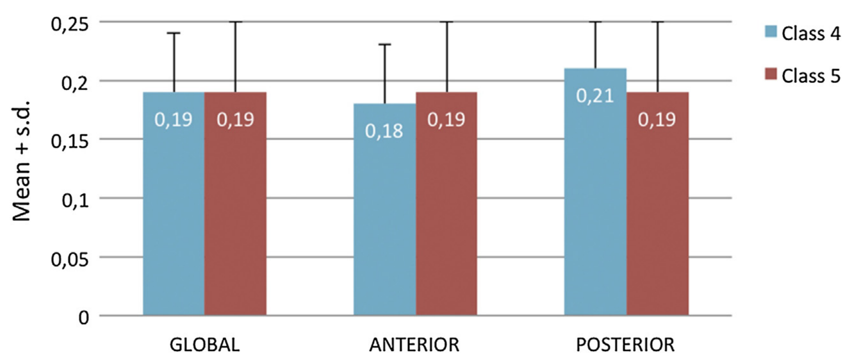

Fig. 17. Volume of malar bone engaged according to the Cawood and Howell classification of alveolar bone atrophy (classes IV and V), in cubic centimetres.

spectively) (Table 2). The results are illustrated in Fig. 17.

Intra-malar implant length

The mean intra-malar length for the total sample of 92 implants was 16.95 ± 4.73 mm. The intra-malar length of the zygoma implant according to the implant position (anterior or posterior) is shown in Table 3. In the anterior sector ($n = 46$ anterior implants), the mean length of zygomatic implants situated within the malar bone was 17.42 ± 3.74 mm. When categorized according to the Cawood and Howell classification of alveolar bone atrophy, the average intra-malar length was 17.97 ± 4.14 mm in class IV and 16.81 ± 3.24 mm in class V. In the posterior sector ($n = 46$ posterior implants), the average length of the zygomatic implant found within the malar bone was 16.48 ± 5.55 mm. When categorized according to the Cawood and Howell classification of alveolar bone atrophy, the average intra-malar length was 18.51 ± 6.36 mm in class IV and 14.78 ± 4.16 mm in class V. Thus, the mean intra-malar length was greater in class IV than in class V cases.

On comparing the zygoma implant intra-malar length between class IV and class V bone atrophy cases, a statistically significant difference was found for the posterior sector ($P = 0.028$) and for the total sample ($P = 0.011$). These results are summarized in Table 4 and are illustrated in Fig. 18.

Relationship of the zygoma implant to the sinus

According to the Cawood and Howell classification of alveolar bone atrophy

Of the whole sample of 92 implants, 60.9% had an extrasinus path ($n = 56$), 25% a parasinus path ($n = 23$), and the remaining 14.1% had an intrasinus path ($n = 13$), according to the parameters described in the Materials and methods section (Table 5).

With regard to the class of alveolar bone atrophy, the following findings were noted (Table 5): for class IV, of the whole sample of 45 implants, 77.8% had an extrasinus path ($n = 35$), 15.6% had a parasinus path ($n = 7$), and 6.7% had an intrasinus path ($n = 3$); for class V, of the whole sample of 47 implants, 44.7% had an extrasinus path ($n = 21$), 34.0% had a parasinus path ($n = 16$), and 21.3% had an

Table 1. Volume of malar bone (cm^3) engaged by the zygoma implant according to the sector (anterior and posterior) and the Cawood and Howell classification of alveolar bone atrophy (classes IV and V).

	Sector								
	Total			Anterior			Posterior		
	Total	Class IV	Class V	Total	Class IV	Class V	Total	Class IV	Class V
Implants, *n*	92	45	47	46	24	22	46	21	25
Mean	0.19	0.19	0.19	0.18	0.18	0.19	0.20	0.21	0.19
Standard deviation	0.06	0.05	0.06	0.05	0.05	0.06	0.06	0.06	0.06
Minimum	0.10	0.11	0.10	0.11	0.11	0.12	0.10	0.14	0.10
Maximum	0.39	0.34	0.39	0.39	0.28	0.39	0.34	0.34	0.32
Median	0.18	0.18	0.17	0.17	0.17	0.17	0.19	0.20	0.17

Table 3. Zygoma implant intra-malar length (mm) according to the sector (anterior and posterior) and the Cawood and Howell classification of alveolar bone atrophy (classes IV and V).

	Sector								
	Total			Anterior			Posterior		
	Total	Class IV	Class V	Total	Class IV	Class V	Total	Class IV	Class V
Implants, *n*	92	45	47	46	24	22	46	21	25
Mean	16.95	18.22	15.73	17.42	17.97	16.81	16.48	18.51	14.78
Standard deviation	4.73	5.24	3.86	3.74	4.14	3.24	5.55	6.36	4.16
Minimum	9.26	9.79	9.26	12.14	12.14	12.92	9.26	9.79	9.26
Maximum	30.22	30.22	26.43	26.52	26.52	23.76	30.22	30.22	26.43
Median	15.82	17.70	14.50	16.52	17.19	15.79	14.27	19.63	13.56

intrasinus path ($n = 10$). The results are illustrated in Fig. 19.

The association χ^2 test confirmed that the difference in the path of the implant according to the degree of alveolar bone atrophy was statistically significant ($P = 0.005$).

The relationship of the zygoma implant to the sinus (intrasinus, parasinus, or extrasinus) according to the sector (anterior and posterior) is shown in Table 6. In the anterior sector, all cases (100% of the sample) classified as class IV ($n = 24$) had an extrasinus path, compared to 72.7% ($n = 16$) of class V cases; the difference was statistically significant ($P = 0.025$, Kruskal–Wallis test). In the posterior sector, a very strong trend towards statistical significance ($P = 0.067$, χ^2 test) was also detected: in the class IV group, 52.4% had an extrasinus path compared to only 20% in the class V group.

Hence, as the degree of alveolar bone atrophy increases, the implant is more related to the maxillary sinus, acquiring a parasinus or intrasinus path.

According to the Cawood and Howell classification of alveolar bone atrophy and the residual bone height to the floor of the maxillary sinus and the nasal cavity

Since the Cawood and Howell classification of alveolar bone atrophy is based on a visual evaluation of the residual alveolar ridge and can therefore be subjective, an attempt was made to objectively quantify the residual bone. To this effect, the residual alveolar bone height to the floor of the maxillary sinus and the nasal cavity in the respective positions of the zygoma implants was measured. In this way, class IV and class V alveolar bone atrophy were related to a specific quantifiable residual alveolar bone height.

In the assessment of the residual bone height to the floor of the sinus ($n = 46$ implants), a mean overall residual alveolar bone height of 5.83 ± 3.00 mm was measured. When assessed by Cawood and Howell classification, the mean residual alveolar bone height for class IV was 7.85 ± 1.99 mm, while for class V this was reduced to 4.05 ± 2.59 mm.

In the assessment of the residual bone height to the floor of the nasal cavity ($n = 46$ implants), a mean overall residual alveolar bone height of 9.63 ± 4.07 mm was found. When assessed by Cawood and Howell classification, the residual bone height for class IV was a mean 12.64 ± 2.92 mm, while this height was reduced to a mean of 6.48 ± 2.33 mm for class V.

These data are displayed in Table 7 and illustrated in Fig. 20.

Regarding the residual bone height, intrasinus and parasinus paths were found to correspond to lower mean residual bone heights to the maxillary sinus (5.39 ± 2.34 mm and 4.74 ± 2.99 mm, respectively) than extrasinus paths (7.34 ± 2.93 mm). A Kruskal–Wallis test confirmed that the difference was statistically significant ($P = 0.036$).

Similar results were obtained with respect to the residual bone height to the floor of the nasal cavity: an extrasinus path was associated with a higher mean residual bone height ($P = 0.005$, Kruskal–Wallis test).

Focusing on the class of alveolar bone atrophy, only the residual bone height to the floor of the sinus showed similar results for class IV, and the results did not reach statistical significance ($P = 0.260$, Kruskal–Wallis test). For class V, neither the residual bone height to the floor of the sinus ($P = 0.486$, Kruskal–Wallis test) nor the residual bone height to the floor of the nasal cavity ($P = 0.230$, Kruskal–Wallis test) showed significant results.

Hence, the differences in the path of the implant are perceived globally, but not within each degree of bone atrophy. It must be acknowledged that the samples for each subgroup of bone atrophy were relatively small and the statistical power is thereby reduced. The data are displayed in Table 8.

Table 4. Zygoma implant intra-malar length (mm) according to the sector (anterior and posterior) and the Cawood and Howell classification of alveolar bone atrophy (classes IV and V).[a]

	Class IV	Class V	*P*-value[b]
Total	18.2 ± 5.2 (16.6–19.8)	15.7 ± 3.9 (14.6–16.9)	0.011*
Anterior sector	17.9 ± 4.1 (16.2–19.7)	16.8 ± 3.2 (15.4–18.2)	0.297
Posterior sector	18.5 ± 6.4 (15.6–21.4)	14.8 ± 4.2 (13.1–16.5)	0.028*

* Significant difference.
[a] Results are presented as the mean ± standard deviation (95% confidence interval).
[b] The *t*-test was used to compare the means according to the degree of alveolar bone atrophy.

Discussion

The purpose of this study was to investigate the amount of malar bone volume and length that a zygomatic implant can engage and the expected relationship of the implant to the sinus depending on the degree of alveolar bone atrophy. The absence of similar studies in the scientific literature hinders comparisons with the observations of other study groups.

Balshi et al. evaluated malar bone-to-implant contact (BIC) in zygomatic implants[15]. They found a BIC of 15.5 ± 6.0 mm in men and 14.7 ± 5.4 mm in women. These lengths in millimetres correspond to the amount of implant within the malar bone. In the present study, the mean intra-malar length for the total sample was 16.95 ± 4.73 mm. No differentiation was made between men and women; rather, the sample was categorized according to the class of alveolar bone atrophy. In this regard, it was found that the mean intra-malar length in class IV cases was 18.22 ± 5.24 mm and in class V cases was 15.73 ± 3.86. Hence, the average intra-malar length is greater in positions with class IV atrophy than in those with class V atrophy. Nevertheless, statistical significance was reached only

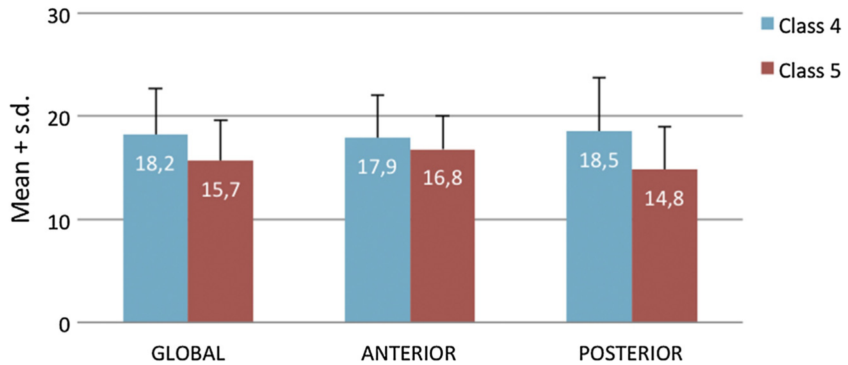

Fig. 18. Intra-malar length according to the Cawood and Howell classification of alveolar bone atrophy (classes IV and V), in millimetres.

Table 5. Relationship of the zygoma implant to the sinus (intrasinus, parasinus, or extrasinus) according to the Cawood and Howell classification of alveolar bone atrophy (classes IV and V).

	Alveolar bone atrophy					
	Total		Class IV		Class V	
	Implants, *n*	%	Implants, *n*	%	Implants, *n*	%
Total	92	100.0%	45	100.0%	47	100.0%
Intrasinus	13	14.1%	3	6.7%	10	21.3%
Parasinus	23	25.0%	7	15.6%	16	34.0%
Extrasinus	56	60.9%	35	77.8%	21	44.7%

for the posterior sector ($P = 0.028$) and the total sample ($P = 0.011$).

Balshi et al. stated that the zygoma BIC varies according to the angle at which the implant is placed. As the angle of the implant placement changes, the implant contacts different anatomical portions of the zygoma, and this can lead to an increase or decrease in the BIC. In the present study, anterior or posterior positioning and the different classes of alveolar bone atrophy changed the angulation of the implant and confirmed this hypothesis with statistical evidence. Similarly, the present results regarding the intra-malar implant length are comparable to those published by Balshi et al.[15], with a discrepancy of 1.65 mm. This small difference may be attributable to several factors, which include the fact that Balshi et al. performed measurements at the lowermost part of the implant in contact with the malar bone, while in the present study the longitudinal implant axis was used. In addition, it must be taken into account that in the study methodology, implant planning was done virtually and it was possible to select the ideal position three-dimensionally in terms of the maximum bone contact. Determining this optimal placement in vivo is not that simple.

It is well acknowledged that the length of the implant located in bone is a key factor in determining osseointegration and the success and survival of the implant. Authors refer to this factor in terms of a 2D linear measurement of an implant that nevertheless has a three-dimensional (3D) volume and is placed into a 3D anatomical structure – the bone. Hence, it seems much more reasonable to talk in 3D terms than in 2D terms. It is surprising, therefore, that the volume of bone engaged by a zygoma implant or a conventional implant has not been covered by previous investigations in the scientific literature.

The data from this study showed that the average volume of malar bone engaged by a zygoma implant was 0.19 ± 0.06 cm^3, with no statistically significant difference whether the implants were placed anteriorly or posteriorly ($P = 0.559$ and $P = 0.184$, respectively), and regardless of the degree of alveolar bone atrophy in the area to be treated ($P = 0.650$). It can, therefore, be concluded that the volume engaged is constant, regardless of the degree of alveolar bone atrophy or position. In other words, despite severe alveolar bone atrophy, the amount of bone volume that the malar bone offers for zygoma implant anchorage is stable and thus renders this therapeutic option reasonable and reliable[14,16–20].

Regarding the relationship of the zygoma implant to the sinus, only one article published by Aparicio reported the relationship of this to the anterior maxillary wall[11]. A description of the morphology of the anterior maxillary wall according to the different degrees of concavity, defined as flat, slightly concave, concave, very concave, and extreme alveolar lateral and vertical bone atrophy, was given, in what the author called the zygoma anatomy guided approach (ZAGA) classification. However, despite the widespread use of the Cawood and Howell classification of alveolar bone atrophy in this field, no relationship between the path of the implant and the different bone atrophy classes was established. In the present study, an important finding was the fact that the relationship of the zygoma implant to the sinus changes depending on the degree of bone atrophy. Indeed, more extrasinus/extramaxillary paths were found for the lower degrees of atrophy than for the higher degrees of atrophy (77.8% for Cawood and Howell class IV compared to 44.7% for Cawood and Howell class V). Hence, as alveolar bone atrophy increases,

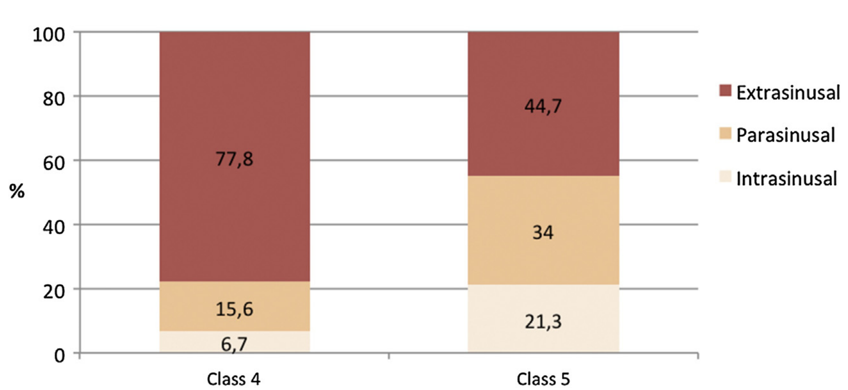

Fig. 19. Zygoma implant path (extrasinus, parasinus, and intrasinus) according to the Cawood and Howell classification of alveolar bone atrophy (classes IV and V).

Table 6. Relationship of the zygoma implant to the sinus (intrasinus, parasinus, or extrasinus) according to the sector (anterior and posterior) and the Cawood and Howell classification of alveolar bone atrophy (classes IV and V).

	Sector								
	Total			Anterior			Posterior		
	Total Implants, *n* (%)	Class IV Implants, *n* (%)	Class V Implants, *n* (%)	Total Implants, *n* (%)	Class IV Implants, *n* (%)	Class V Implants, *n* (%)	Total Implants, *n* (%)	Class IV Implants, *n* (%)	Class V Implants, *n* (%)
Total	92 (100)	45 (100)	47 (100)	46 (100)	24 (100)	22 (100)	46 (100)	21 (100)	25 (100)
Intrasinus	13 (14.1)	3 (6.7)	10 (21.3)	2 (4.3)	0 (0)	2 (9.1)	11 (23.9)	3 (14.3)	8 (32)
Parasinus	23 (25.0)	7 (15.6)	16 (34.0)	4 (8.7)	0 (0)	4 (18.2)	19 (41.3)	7 (33.3)	12 (48)
Extrasinus	56 (60.9)	35 (77.8)	21 (44.7)	40 (87.0)	24 (100)	16 (72.7)	16 (34.8)	11 (52.4)	5 (20)

Table 7. Residual height (mm) to the floor of the maxillary sinus and the nasal cavity in the location of the zygoma implant according to the Cawood and Howell classification of alveolar bone atrophy (classes IV and V).

	Alveolar bone atrophy		
	Total	Class IV	Class V
Height to sinus floor			
Implants, *n*	46	21	25
Mean	5.83	7.85	4.05
Standard deviation	3.00	1.99	2.59
Minimum	1.00	3.03	1.00
Maximum	11.97	11.97	9.30
Median	6.39	7.81	3.86
Height to nasal cavity			
Implants, *n*	46	24	22
Mean	9.63	12.64	6.48
Standard deviation	4.07	2.92	2.33
Minimum	1.92	7.53	1.92
Maximum	18.43	18.43	11.77
Median	9.02	12.67	6.73

the relationship to the sinus tends towards a more intrasinus path.

Another factor influencing the relationship of the zygoma implant to the sinus is the residual alveolar bone height to the floor of the nasal cavity and the maxillary sinus. More intrasinus/intramaxillary paths were found for lower residual alveolar bone heights. Thus, as the residual bone height increases, the relationship of the implant to the sinus tends towards a more extrasinus/extramaxillary path.

In conclusion, the results of this study suggest that the average volume of malar bone that a zygoma implant engages is 0.19 ± 0.06 cm^3. This amount does not vary regardless of the implant position and degree of alveolar bone atrophy. All of the cases evaluated showed enough bone volume at the zygoma level to allow for quadruple implant placement. In none of the cases did the examiners fail to find sufficient bone to adequately distribute the implants. Although it was not the purpose of this study, from this experience in the virtual scenario, it can be hypothesized that any malar bone is actually appropriate for the placement of two fixtures.

As the degree of alveolar bone atrophy increases, the path of the zygomatic implant becomes more parasinus and intrasinus.

The absence of similar studies in the scientific literature limits the establishment of comparisons with other study groups. Further investigations should incorporate state-of-the-art imaging technologies and 3D implant parameters such as minimum alveolar bone volume engagement required for successful osseointegration.

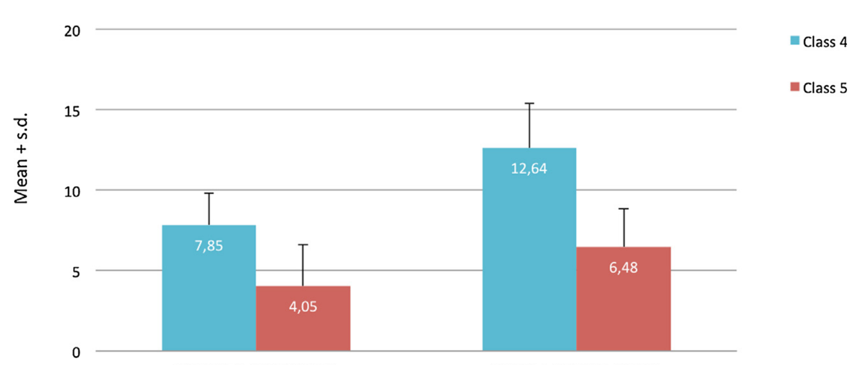

Fig. 20. Residual bone height to the floor of the maxillary sinus and to the floor of the nasal cavity according to the Cawood and Howell classification of alveolar bone atrophy (classes IV and V).

Please cite this article in press as: Bertos J, et al. Virtual quad zygoma implant placement using cone beam computed tomography: sufficiency of malar bone volume, intraosseous implant length, and relationship to the sinus according to the degree of alveolar bone

Table 8. Relationship of the zygoma implant to the sinus (intrasinus, parasinus, or extrasinus) according to the Cawood and Howell classification of alveolar bone atrophy (classes IV and V) and the residual bone height to the floor of the maxillary sinus and the nasal cavity.

	Total alveolar bone atrophy				Class IV alveolar bone atrophy				Class V alveolar bone atrophy			
	Relation to the sinus				Relation to the sinus				Relation to the sinus			
	Total	Intra	Para	Extra	Total	Intra	Para	Extra	Total	Intra	Para	Extra
Height to sinus floor												
Implants, *n*	46	11	19	16	21	3	7	11	25	8	12	5
Mean	5.83	5.39	4.74	7.34	7.85	8.18	6.64	8.53	4.05	4.35	3.53	4.73
Standard deviation	3.00	2.34	2.99	2.93	1.99	1.25	1.96	1.93	2.59	1.67	2.95	3.22
Minimum	1.00	2.00	1.00	1.00	3.03	6.77	3.03	6.39	1.00	2.00	1.00	1.00
Maximum	11.97	9.14	9.30	11.97	11.97	9.14	8.70	11.97	9.30	6.73	9.30	8.64
Average	6.39	4.90	5.70	7.22	7.81	8.62	7.69	8.56	3.86	4.69	2.00	5.12
Height to nasal cavity												
Implants, *n*	46	2	4	40	24	0	0	24	22	2	4	16
Mean	9.63	5.58	5.18	10.39	12.64	–	–	12.64	6.48	5.58	5.18	7.00
Standard deviation	4.07	2.76	1.10	3.90	2.02	–	–	2.92	2.33	2.76	1.10	2.48
Minimum	1.92	3.62	3.94	1.92	7.53	–	–	7.53	1.92	3.62	3.94	1.92
Maximum	18.43	7.53	6.73	18.43	18.43	–	–	18.43	11.77	7.53	6.73	11.77
Average	9.02	5.58	4.82	10.17	12.67	–	–	12.67	6.73	5.58	4.82	7.15

Funding

None.

Competing interests

None.

Ethical approval

The Research Ethic Committee (C.E.R.) of the International University of Catalonia approved this research (reference number CIR-ELM-2013-02).

Patient consent

Not required.

Acknowledgements. Special thanks to Gemma Puerta López-Pastor for her great dedication and contribution to this study, to Juan Luís Gómez Martínez for assistance with the statistical analysis, and to Marina Monjó and Simplant (Dentsply Sirona, Iberia) for the technical support in the use of the software.

References

1. Brånemark P. *Surgery and fixture installation: zygomaticus fixture clinical procedures*. First edition. Goteborg, Sweden: Nobel Biocare AB; 1998.
2. Stella JP, Warner MR. Sinus slot technique for simplification and improved orientation of zygomaticus dental implants: a technical note. *Int J Oral Maxillofac Implants* 2000;**15**:889–93.
3. Maló M, de Araujo Nobre E, Lopes I. A new approach to rehabilitate the severely atrophic maxilla using extramaxillary anchored implants in immediate function: a pilot study. *J Prosthet Dent* 2008;**100**:354–66.
4. Ramos Chrcanovic B, Ribeiro Pedrosa A, Neto Custódio A. Zygomatic implants: a critical review of the surgical techniques. *Oral Maxillofac Surg* 2013;**17**:1–9.
5. Bothur S, Garsten M. Initial speech problems in patients treated with multiple zygomatic implants. *Int J Oral Maxillofac Implants* 2010;**25**:379–84.
6. Aparicio C, Ouazzani W, Aparicio A, Fortes V, Muela R, Pascual A, Codesal M, Barluenga N, Manresa C, Franch M. Extrasinus zygomatic implants: three year experience from a new surgical approach for patients with pronounced buccal concavities in the edentulous maxilla. *Clin Implant Dent Relat Res* 2010;**12**:55–61.
7. Malo P, Nobre M, Lopes A, Francischone C, Rigolizzo M. Three-year outcome of a retrospective cohort study on the rehabilitation of completely edentulous atrophic maxillae with immediately loaded extra-maxillary zygomatic implants. *Eur J Oral Implantol* 2012;**5**:37–46.
8. Aparicio C, Manresa C, Francisco K, Claros P, Alandez J, Gonzalez-Martin O, Albrektsson T. Zygomatic implants: indications, techniques and outcomes, and the zygomatic success code. *Periodontol 2000* 2014;**66**:41–58.
9. Peñarrocha M, García B, Martí E, Boronat A. Rehabilitation of severely atrophic maxillae with fixed implant-supported prostheses using zygomatic implants placed using the sinus slot technique: clinical report on a series of 21 patients. *Int J Oral Maxillofac Implants* 2007;**22**:645–50.
10. Chrcanovic BR, Nogueira Guimarães Abreu MH. Survival and complications of zygomatic implants: a systematic review. *Oral Maxillofac Surg* 2013;**17**:81–93.
11. Aparicio C. A proposed classification for zygomatic implant patient based on the zygoma anatomy guided approach (ZAGA): a cross-sectional survey. *Eur J Oral Implantol* 2011;**4**:269–75.
12. Cawood J, Howell R. A classification of the edentulous jaws. *Int J Oral Maxillofac Surg* 1988;**17**:232–6.
13. Rossi M, Duarte LR, Mendonca R, Fernandes A. Anatomical bases for the insertion of zygomatic implants. *Clin Implant Dent Relat Res* 2008;**10**:271–5.
14. Rigolizzo M, Camilli J, Francischone C, Padovani C, Brånemark P. Zygomatic bone: anatomic bases for osseointegrated implant anchorage. *Int J Oral Maxillofac Implants* 2005;**20**:441–7.
15. Balshi TJ, Wolfinger GJ, Shuscavage NJ, Balshi SF. Zygomatic bone-to-implant contact in 77 patients with partially or completely edentulous maxillas. *J Oral Maxillofac Surg* 2012;**70**:2065–9.
16. Stiévenart M, Malevez C. Rehabilitation of totally atrophied maxilla by means of four zygomatic implants and fixed prosthesis: a 6-40-month follow-up. *Int J Oral Maxillofac Surg* 2010;**39**:358–63.
17. Davó R, Pons O. Prostheses supported by four immediately loaded zygomatic implants: a 3-year prospective study. *Eur J Oral Implantol* 2013;**6**:262–9.
18. Aparicio C, Manresa C, Francisco K, Ouazzani W, Claros P, Potau J, Aparicio A. The long-term use of zygomatic implants: a 10-year clinical and radiographic report. *Clin Implant Dent Relat Res* 2014;**16**:447–59.
19. Malevez C. Zygomatic anchorage concept in full edentulism. *Rev Stomatol Chir Maxillofac* 2012;**113**:299–306. http://dx.doi.org/10.1016/jstomax201206001.
20. Davó R, Pons O. 5-year outcome of cross-arch prostheses supported by four immediately loaded zygomatic implants: a prospective case series. *Eur J Oral Implantol* 2015;**8**:169–74.

Address:
Jorge Bertos Quílez
Department of Oral and Maxillofacial Surgery
International University of Catalonia
C/Josep Trueta s/n
08195 Sant Cugat del Vallés
Barcelona
Spain
Tel.: +34 687 595 482
E-mail: jorgebertos@uic.es